THREE DIMENSIONAL ANALYSIS OF LAMINATED CYLINDRICAL PANELS WITH PIEZOELECTRIC LAYERS

A. Nosier and M. Ruhi*

Department of Mechanical Engineering, Sharif University of Technology
Tehran, Iran
Nosier@sharif.edu - Mohammad_Ruhi@yahoo.com

*Corresponding Author

(Received: November 18, 2004 - Accepted in Revised Form: June 1, 2006)

Abstract A semi-analytical solution is presented for three dimensional elastic analysis of finitelylong, simply supported, orthotropic, laminated cylindrical panels with piezoelectric layers subjected to outer pressure and electrostatic excitation. Both the direct and inverse piezoelectric effects are investigated. The solution is obtained through reducing the highly coupled partial differential equations (PDE's) of equilibrium to ordinary differential equations (ODE's) with variable coefficients by means of trigonometric function expansion in longitudinal and circumferential directions. The resulting ODE's are solved by dividing the radial domain into some finite subdivisions and imposing necessary continuity conditions between the adjacent sub-layers. Some numerical examples are presented for the stress distribution and electric responses due to outer pressure in both sensorial and actuating states. Also, the effect of geometric properties on the sensitivity and actuating power of the structure are investigated.

Key Words Piezoelectric, Laminated Cylindrical Panel, Finite, Analytical

چکیده در این مقاله یک روش نیمه تحلیلی برای حل معادلات الاستیک حاکم بر یک قطاع استوانه ای مرکب چندلایه با لایه های پیزوالکتریک و طول محدود قرار گرفته در معرض بارگذاری مکانیکی و الکتریکی ارائه گردیده است. اثر مستقیم و معکوس پیزوالکتریک در ارائه روش حل و نتایج مورد بررسی قرار گرفته است. ابتدا با استفاده از بسط فوریه در دو راستای طولی ومحیطی، معادلات تعادل حاکم بر محیط که از نوع معادلات دیفرانسیل پاره ای می‌باشند به یک دسته معادله دیفرانسیل معمولی با ضرایب متغیر (وابسته به مختصات شعاعی) کاهش داده می‌شوند. سپس با تقسیم محدوده شعاعی به تعدادی لایه های نازک و محاسبه ضرایب معادلات دیفرانسیل معمولی به دست آمده در آن نواحی، این معادلات به معادلاتی با ضرایب ثابت تبدیل می‌شوند. با اعمال شرایط پیوستگی ضروری بین لایه های فرضی در مجاورت یکدیگر پاسخ ها در هر ناحیه به صورت توابع نمایی بر حسب مختصات شعاعی به دست خواهد آمد. در پایان، نتایج عددی به دست آمده برای هر دو حالت حسگری و عملگری مورد بررسی قرار گرفته است. همچنین اثرات مربوط به ویژگی های هندسی سازه، بر روی میزان حساسیت و قدرت عملگری آن مورد بحث و بررسی قرار گرفته است.

1. INTRODUCTION

Piezoelectricity was first discovered by Jacques and Pierre Curie in 1880, and other materials later discovered included rochelle salt ($NaKC_2H_4O_6.4H_2O$), barium titanate ($BaTiO_3$), lead titanate ($PbTiO_3$), lead zirconate titanate ($PbZr_{0.52}Ti_{0.48}O_3$), zinc oxide (ZnO), aluminum nitride (AlN), polyvinyliden fluoride (PVDF) and its copolymers with trifluoroethylene (TrFE) and tetraflouoroethylene (TFE), etc. Since lead zirconate titanate (PZT) has excellent piezoelectric properties, a high Curie temperature, high spontaneous polarization and high electromechanical coupling coefficient, it is probably the most widely used piezoelectric material. On the other hand, light and flexible ferroelectric polymers, especially PVDF, show many advantages over ceramics for several applications. So, composites made of ferroelectric ceramics combined with polymers have several advantages over pure piezoelectric materials. Therefore, Diphasic composites of PZT (and La/Ca modified PZT) combined with various polymers such as PVDF, PVC, PVA, epoxy resin and co-polymers have been widely studied and reported in

the literature. Several intelligent composite material systems, combining piezoelectric materials with structural materials, have received attention in various industrial fields. The mechanics of laminated piezoelectric structures therefore has gained much attention [1-5]. There are two characteristics of piezoelectric materials which permit them to be used as sensors and actuators. One is their direct piezoelectric effect which implies that the materials induce electric charge or electric potential when they are subjected to mechanical deformations. Conversely, the second effect happens when they are deformed if some electric charge or electric potential is imposed on them, which is called inverse piezoelectric effect. Laminated composite shells with piezoelectric layers are important components of smart or intelligent structures. Analytical three-dimensional studies for these structures are not only valuable in their own right, but they are also useful for studying various approximate theories and computational models.

Mitchell and Reddy [6] have presented a power series solution for the static analysis of an axisymmetric composite cylinder with surface bonded or embedded piezoelectric lamina. Chen and his coworkers [7-9] have developed a variety of analytical and approximate solutions for piezoelectric shells. A higher order theory for functionally graded piezoelectric shells has been developed by Wu and his coworkers [10]. Wang and Zhong [11] investigated analytically the problem of a finitely long circular cylindrical shell of cylindrically orthotropic piezoelectric/piezomagnetic composite under pressure loading and a uniform temperature change. They obtained an analytical solution through the power series expansion method and the Fourier series expansion method. Kapuria et al. [12] have presented an exact piezothermoelastic solution of a finite transversely isotropic piezoelectric cylindrical shell under axisymmetric thermal, pressure, and electrostatic excitation by formulating the problem in terms of potential functions and using Fourier expansion series. Ossadzow and Touratier [13] have presented a two-dimensional theory for the analysis of piezoelectric shells based on a hybrid approach in which the continuity conditions for both mechanical and electric unknowns at layer interfaces as well as the imposed conditions on the bounding surfaces and at the interfaces are independently satisfied. Wu and his coworkers [14] have presented an analytical study for piezothermoelastic behavior of a functionally graded piezoelectric cylindrical shell subjected to axisymmetric thermal or mechanical loading. They have used the Fourier series expansion method together with the power series expansion method to reduce the governing PDE's to ODE's and have obtained the solution for both direct and inverse piezoelectric effects. Ma and his coworkers [15] have studied two-dimensional problems of anisotropic cylindrical piezoelectric tube, bar, and shell in a cylindrical coordinate system. They found that the electrical parameters of piezoelectric materials influence the formations of the solution significantly. Some researches on thermoelastic displacement and shape control of the laminated piezoelectric structures are treated in [16-18]. Also Ootao and Tanigawa [19] have analyzed the transient piezothermoelastic problem of an angle-ply laminated cylindrical panel bonded to a piezoelectric layer. They also examined the influence of thickness of angle-ply laminate on the applied electric potential and transverse stresses. Tzou [20] represented a collection of relevant researches and developments on piezoelectric shells and related applications to the distributed measurement and control of continua.

In this study a very simple semi-analytical solution is presented for three-dimensional elasticity equations governing the finite laminated composite cylindrical panels with piezoelectric layers. The laminated panel is subjected to a uniform external pressure and an electric excitation. The panel is supposed to have simple supports at its four edges. The governing elasticity equations are reduced to ordinary differential equations (ODE's) using a doubly periodic solution in the shell surface coordinates. The resulting ODE's are solved by dividing the radial domain to some small finite subdivisions in which the radial coordinate appearing in the coefficients of these ODE's is treated to be constant. A convergence study is then carried out in order to determine the proper number of subdivisions made in each physical layer. Finally numerical results are presented for typical prescribed outer pressure and electric charge excitations in both sensorial and actuating states. Also, the effect of geometric

properties of the cylindrical panel on the sensitivity and actuating power of the structure are studied.

2. FUNDAMENTAL EQUATIONS OF PIEZOELASTICITY

The linear constitutive equations coupling the piezo-elastic field are given by [20]:

$$\sigma_{ij} = C_{ijkl}\varepsilon_{kl} - e_{mij}E_m \quad (1)$$

$$D_i = e_{ikl}\varepsilon_{kl} + \in_{im} E_m \quad (2)$$

where σ_{ij} and ε_{ij} are the stress and strain tensors. Also D_i and E_i are the electric field vectors and C_{ijkl}, e_{mij}, and $\in_{im}$ are the elastic constants, the piezoelectric stress constants, and the piezoelectric coefficients, respectively. Relation 1 denotes the inverse piezoelectric effect while 2 presents the direct piezoelectric effect [20]. It is to be noted that in 1 and 2 a repeated index implies summation from one to three.

The equilibrium equations are given by [20,21]:

$$\sigma_{ij,j} = 0 \quad (3)$$

$$D_{i,i} = 0 \quad (4)$$

The linear relations between the strain components ε_{ij}'s and the displacement components U_i's and the electric field E_i and the electric potential Ψ are given by [20,21]:

$$\varepsilon_{ij} = \frac{1}{2}(U_{i,j} + U_{j,i}) \quad (5)$$

$$E_i = -\Psi_{,i} \quad (6)$$

where an index following a comma indicates partial differentiation with respect to a coordinate.

In this part, a finite laminated cylindrical panel with piezoelectric layers is considered (see Figure 1). The shell to be considered is composed of orthotropic cross-ply layers and some piezoelectric layers while the orthotropic layers are made of reinforced fiber composites.

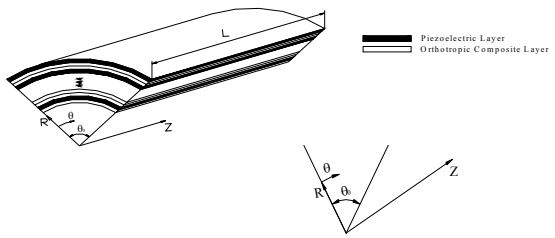

Figure 1. configuration of the laminated cylindrical panel piezoelectric layers.

The panel is subjected to a uniform outer pressure, R_{in} is the inner surface radius and R_{out} is the outer one. For convenience the following variables are introduced

$$(r,z) = \frac{(R,Z)}{R_0}$$
$$(u_r, u_\theta, u_z, \psi) = \frac{(U_R, U_\theta, U_z, \Psi)}{R_0} \quad (7)$$

where R_0 is the middle surface radius of the shell panel. In the cylindrical coordinate system {r, θ, z} Relations 3 to 6 are given as follows [20,21];

Gradient relations:

$$\varepsilon^k{}_z = \frac{\partial u^k{}_z}{\partial z}, \quad \varepsilon^k{}_\theta = \frac{1}{r}\left(\frac{\partial u^k{}_\theta}{\partial \theta} + u^k{}_r\right)$$
$$\varepsilon^k{}_r = \frac{\partial u^k{}_r}{\partial r}$$
$$\gamma^k{}_{\theta z} = \frac{\partial u^k{}_\theta}{\partial z} + \frac{1}{r}\frac{\partial u^k{}_z}{\partial \theta}, \quad \gamma^k{}_{rz} = \frac{\partial u^k{}_z}{\partial r} + \frac{\partial u^k{}_r}{\partial z} \quad (8)$$
$$\gamma^k{}_{r\theta} = \frac{1}{r}\left(\frac{\partial u^k{}_r}{\partial \theta} - u^k{}_\theta + r\frac{\partial u^k{}_\theta}{\partial r}\right)$$

$$E^{kp}{}_r = -\frac{\partial \psi^{kp}}{\partial r}, \quad E^{kp}{}_\theta = -\frac{1}{r}\frac{\partial \psi^{kp}}{\partial \theta}$$
$$E^{kp}{}_z = -\frac{\partial \psi^{kp}}{\partial z} \quad (9)$$

Equilibrium Equations [20,21]:

$$\frac{\partial \sigma^k{}_r}{\partial r}+\frac{(\sigma^k{}_r-\sigma^k{}_\theta)}{r}+\frac{1}{r}\frac{\partial \tau^k{}_{r\theta}}{\partial \theta}+\frac{\partial \tau^k{}_{rz}}{\partial z}=0$$
$$\frac{\partial \tau^k{}_{r\theta}}{\partial r}+\frac{1}{r}\frac{\partial \sigma^k{}_\theta}{\partial \theta}+\frac{\partial \tau^k{}_{z\theta}}{\partial z}+2\frac{\tau^k{}_{r\theta}}{r}=0 \qquad (10)$$
$$\frac{\partial \tau^k{}_{rz}}{\partial r}+\frac{1}{r}\frac{\partial \tau^k{}_{z\theta}}{\partial \theta}+\frac{\partial \sigma^k{}_z}{\partial z}+\frac{\tau^k{}_{rz}}{r}=0$$

$$\frac{\partial D^{kp}{}_r}{\partial r}+\frac{D^{kp}{}_r}{r}+\frac{1}{r}\frac{\partial D^{kp}{}_\theta}{\partial \theta}+\frac{\partial D^{kp}{}_z}{\partial z}=0 \qquad (11)$$

Constitutive Relations A piezoelectric material with symmetrical hexagonal structure (Class C_{6v} = 6 mm) exhibits transverse isotropy about its third axis. Therefore, the constitutive relations for piezoelectric layers are [21];

$$\begin{Bmatrix}\sigma_r\\ \sigma_\theta\\ \sigma_z\\ \tau_{\theta z}\\ \tau_{rz}\\ \tau_{r\theta}\end{Bmatrix}^k=\begin{bmatrix}C_{11} & C_{12} & C_{13} & 0 & 0 & 0\\ & C_{22} & C_{23} & 0 & 0 & 0\\ & & C_{33} & 0 & 0 & 0\\ & & & C_{44} & 0 & 0\\ & \text{Sym.} & & & C_{55} & 0\\ & & & & & C_{66}\end{bmatrix}^k\begin{Bmatrix}\varepsilon_r\\ \varepsilon_\theta\\ \varepsilon_z\\ \gamma_{\theta z}\\ \gamma_{rz}\\ \gamma_{r\theta}\end{Bmatrix}^k \qquad (12)$$
$$-\begin{bmatrix}e_{33} & 0 & 0\\ e_{31} & 0 & 0\\ e_{32} & 0 & 0\\ 0 & 0 & 0\\ 0 & 0 & e_{24}\\ 0 & e_{15} & 0\end{bmatrix}^{kp}\begin{Bmatrix}E_r\\ E_\theta\\ E_z\end{Bmatrix}^{kp}$$

and

$$\begin{Bmatrix}D_r\\ D_\theta\\ D_z\end{Bmatrix}^{kp}=\begin{bmatrix}e_{33} & e_{31} & e_{32} & 0 & 0 & 0\\ 0 & 0 & 0 & 0 & 0 & e_{15}\\ 0 & 0 & 0 & 0 & e_{24} & 0\end{bmatrix}^{kp}\begin{Bmatrix}\varepsilon_r\\ \varepsilon_\theta\\ \varepsilon_z\\ \gamma_{\theta z}\\ \gamma_{rz}\\ \gamma_{r\theta}\end{Bmatrix}^{kp} \qquad (13)$$
$$+\begin{bmatrix}\in_{33} & 0 & 0\\ 0 & \in_{11} & 0\\ 0 & 0 & \in_{22}\end{bmatrix}^{kp}\begin{Bmatrix}E_r\\ E_\theta\\ E_z\end{Bmatrix}^{kp}$$

It is to be noted that in 8 through 13 the index k denotes the k^{th} layer and index kp denotes the k^{th} layer which is piezoelectric. That is, for non-piezoelectric layers Equations 9, 11, and 13 disappear and the last term in Equation 12 must be dropped (i.e., $e_{ij} = 0$ for composite layers).

The boundary conditions to be considered are those for simple supports [21,22];

$$u_r=u_\theta=\sigma_z=\psi=0 \qquad \text{at} \quad z=0,\frac{L}{R_0} \qquad (14)$$
$$u_r=u_z=\sigma_\theta=\psi=0 \qquad \text{at} \quad \theta=0,\theta_0$$

The traction conditions on the inner and outer surfaces are assumed to be as follows;

$$\sigma_r=\tau_{r\theta}=\tau_{rz}=0 \qquad \text{at} \qquad r=\frac{R_{in}}{R_0} \qquad (15)$$
$$\sigma_r=-q_0\ ,\ \ \tau_{r\theta}=\tau_{rz}=0 \qquad \text{at} \qquad r=\frac{R_{out}}{R_0}$$

In addition, any piezoelectric layer electrical boundary conditions must be satisfied [22];

$$\psi^{kp}=0 \qquad \text{at} \qquad r=\frac{R^{kp}_{in}}{R_0} \qquad (16)$$

where R^{kp}_{in} is the inner surface radius of the k^{th} piezoelectric layer. Furthermore;

$$\psi^{kp}=V_0 \qquad \text{at} \qquad r=\frac{R^{kp}_{out}}{R_0} \qquad (17a)$$

if the piezoelectric layer is used as an actuator and

$$D^{kp}{}_r=0 \qquad \text{at} \qquad r=\frac{R^{kp}_{out}}{R_0} \qquad (17b)$$

if the piezoelectric layer is served as a sensor where R^{kp}_{out} is the outer surface radius of the k^{th} piezoelectric layer.

It should be mentioned that when a piezoelectric layer is served as an actuator, a voltage is imposed on one of the surfaces of the piezoelectric lamina and the other surface is in zero voltage level, while it serves as a sensor, one surface of the piezoelectric layer is free of electric excitation and the other one is in zero voltage level

as formulated in the above.

3. METHOD OF ANALYSIS

The following expansions are used for various response quantities;

$$
\begin{aligned}
u^k_r &= \sum_{m=1}^{\infty}\sum_{n=1}^{\infty} \Phi^k_r \sin\alpha_m\theta.\sin\beta_n z \\
u^k_\theta &= \sum_{m=1}^{\infty}\sum_{n=1}^{\infty} \Phi^k_\theta \cos\alpha_m\theta.\sin\beta_n z \\
u^k_z &= \sum_{m=1}^{\infty}\sum_{n=1}^{\infty} \Phi^k_z \sin\alpha_m\theta.\cos\beta_n z \\
\psi^{kp} &= \sum_{m=1}^{\infty}\sum_{n=1}^{\infty} \psi^{kp} \sin\alpha_m\theta.\sin\beta_n z
\end{aligned}
\tag{18a}
$$

where $\Phi^k_r, \Phi^k_\theta, \Phi^k_z$ and ψ^{kp} are functions of "r" only, the index k implies the k^{th} orthotropic layer, the index kp implies the k^{th} piezoelectric layer, and

$$
\alpha_m = \frac{m\pi}{\theta_0} \quad , \quad \beta_n = \frac{n\pi R_0}{L} \tag{18b}
$$

Substituting Equations 18a into gradient Equations 8 and 9 and the subsequent results into the constitutive Relations 12 and 13 and the final results into the equilibrium Equations 10 and 11 yields;

$$
\begin{aligned}
&\{C^k_{11}\frac{d^2}{dr^2}+\frac{C^k_{11}}{r}(\frac{d}{dr})-(\frac{C^k_{22}}{r^2}+\frac{C^k_{66}}{r^2}\alpha^2_m+C^k_{55}\beta^2_n)\}\Phi^k_r \\
&+\{-\frac{\alpha_m}{r}(C^k_{12}+C^k_{66})\frac{d}{dr}+\frac{\alpha_m}{r^2}(C^k_{22}+C^k_{66})\}\Phi^k_\theta \\
&+\{-\beta_n(C^k_{13}+C^k_{55})\frac{d}{dr}+\frac{\beta_n}{r}(C^k_{23}-C^k_{13})\}\Phi^k_z \\
&+\{e^{kp}_{33}\frac{d^2}{dr^2}+\frac{1}{r}(e^{kp}_{33}-e^{kp}_{31})\frac{d}{dr}-(\frac{\alpha^2_m}{r^2}e^{kp}_{15}+\beta^2_n e^{kp}_{24})\}\psi^{kp}=0
\end{aligned}
\tag{19}
$$

$$
\begin{aligned}
&\{\frac{\alpha_m}{r}(C^k_{66}+C^k_{21})\frac{d}{dr}+\frac{\alpha_m}{r^2}(C^k_{22}+C^k_{66})\}\Phi^k_r \\
&+\{C^k_{66}\frac{d^2}{dr^2}+\frac{C^k_{66}}{r}\frac{d}{dr}-(\frac{C^k_{66}}{r^2}+\alpha^2_m r^2 C^k_{22}+\beta^2_n C^k_{44})\}\Phi^k_\theta \\
&+\{-\frac{\alpha_m\beta_n}{r}(C^k_{23}+C^k_{44})\}\Phi^k_z \\
&+\{\frac{\alpha_m}{r}(e^{kp}_{15}+e^{kp}_{31})\frac{d}{dr}+\frac{\alpha_m}{r^2}e^{kp}_{15}\}\psi^{kp}=0
\end{aligned}
\tag{20}
$$

$$
\begin{aligned}
&\{\beta_n(C^k_{55}+C^k_{31})\frac{d}{dr}+\frac{\beta_n}{r}(C^k_{32}+C^k_{55})\}\Phi^k_r \\
&+\{-\frac{\alpha_m\beta_n}{r}(C^k_{44}+C^k_{32})\}\Phi^k_\theta \\
&+\{C^k_{55}\frac{d^2}{dr^2}+\frac{C^k_{55}}{r}\frac{d}{dr}-(\frac{\alpha^2_m}{r^2}C^k_{44}+C^k_{33}\beta^2_n)\}\Phi^k_z \\
&+\{\beta_n(e^{kp}_{24}+e^{kp}_{32})\frac{d}{dr}+\frac{\beta_n}{r}e^{kp}_{24}\}\psi^{kp}=0
\end{aligned}
\tag{21}
$$

$$
\begin{aligned}
&\{e^{kp}_{33}\frac{d^2}{dr^2}+\frac{1}{r}(e^{kp}_{31}+e^{kp}_{33})\frac{d}{dr}-(\frac{\alpha^2_m}{r^2}e^{kp}_{15}+\beta^2_n e^{kp}_{24})\}\Phi^k_r \\
&+\{-\frac{\alpha_m}{r}(e^{kp}_{31}+e^{kp}_{15})\frac{d}{dr}+\frac{\alpha_m}{r^2}e^{kp}_{15}\}\Phi^k_\theta \\
&+\{-\beta_n(e^{kp}_{32}+e^{kp}_{24})\frac{d}{dr}-\frac{\beta_n}{r}e^{kp}_{32}\}\Phi^k_z \\
&+\{-e^{kp}_{33}\frac{d^2}{dr^2}-\frac{e^{kp}_{33}}{r}\frac{d}{dr}+(\frac{\alpha^2_m}{r^2}e^{kp}_{11}+\beta^2_n e^{kp}_{22})\}\psi^{kp}=0
\end{aligned}
\tag{22}
$$

The above equations with variable coefficients have been solved by Xu and Noor [23] through a modified Frobenius method. In this study, however, they will be solved by dividing each layer into some finite thin sub-layers as shown in Figure 2.

That is, the k^{th} layer within the laminate is divided into *N* sublayers. This way, since each sublayer becomes very thin, the variable *r* appearing in Equations 19 through 22 can be replaced by the mean radius r_k (n) of each sublayer. The resulting equations will be four ODE's with constant coefficients as follows,

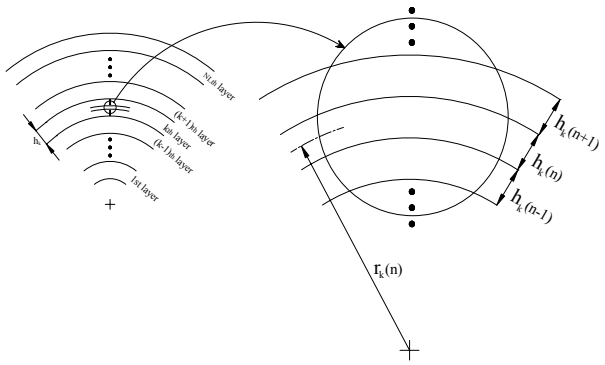

Figure 2. k^{th} layer is divided into N thin sublayers with thickne h_k (n), n = 1, …, N.

$$\{C^k_{11}\frac{d^2}{dr^2}+\frac{C^k_{11}}{r_k(n)}(\frac{d}{dr})-(\frac{C^k_{22}}{r^2_k(n)}+\frac{C^k_{66}}{r^2_k(n)}\alpha^2_m+C^k_{55}\beta^2_n)\}\Phi^k_r$$
$$+\{-\frac{\alpha_m}{r_k(n)}(C^k_{12}+C^k_{66})\frac{d}{dr}+\frac{\alpha_m}{r^2_k(n)}(C^k_{22}+C^k_{66})\}\Phi^k_\theta$$
$$+\{-\beta_n(C^k_{13}+C^k_{55})\frac{d}{dr}+\frac{\beta_n}{r_k(n)}(C^k_{23}-C^k_{13})\}\Phi^k_z \quad (23)$$
$$+\{e^{kp}_{33}\frac{d^2}{dr^2}+\frac{1}{r_k(n)}(e^{kp}_{33}-e^{kp}_{31})\frac{d}{dr}-(\frac{\alpha^2_m}{r^2_k(n)}e^{kp}_{15}+\beta^2_n e^{kp}_{24})\}\psi^{kp}=0$$

$$\{\frac{\alpha_m}{r_k(n)}(C^k_{66}+C^k_{21})\frac{d}{dr}+\frac{\alpha_m}{r^2_k(n)}(C^k_{22}+C^k_{66})\}\Phi^k_r$$
$$+\{C^k_{66}\frac{d^2}{dr^2}+\frac{C^k_{66}}{r_k(n)}\frac{d}{dr}-(\frac{C^k_{66}}{r^2_k(n)}+\alpha^2_m r^2_k(n)C^k_{22}+\beta^2_n C^k_{44})\}\Phi^k_\theta \quad (24)$$
$$+\{-\frac{\alpha_m\beta_n}{r_k(n)}(C^k_{23}+C^k_{44})\}\Phi^k_z$$
$$+\{\frac{\alpha_m}{r_k(n)}(e^{kp}_{15}+e^{kp}_{31})\frac{d}{dr}+\frac{\alpha_m}{r^2_k(n)}e^{kp}_{15}\}\psi^{kp}=0$$

$$\{\beta_n(C^k_{55}+C^k_{31})\frac{d}{dr}+\frac{\beta_n}{r}(C^k_{32}+C^k_{55})\}\Phi^k_r$$
$$+\{-\frac{\alpha_m\beta_n}{r_k(n)}(C^k_{44}+C^k_{32})\}\Phi^k_\theta$$
$$+\{C^k_{55}\frac{d^2}{dr^2}+\frac{C^k_{55}}{r_k(n)}\frac{d}{dr}-(\frac{\alpha^2_m}{r^2_k(n)}C^k_{44}+C^k_{33}\beta^2_n)\}\Phi^k_z \quad (25)$$
$$+\{\beta_n(e^{kp}_{24}+e^{kp}_{32})\frac{d}{dr}+\frac{\beta_n}{r_k(n)}e^{kp}_{24}\}\psi^{kp}=0$$

$$\{e^{kp}_{33}\frac{d^2}{dr^2}+\frac{1}{r_k(n)}(e^{kp}_{31}+e^{kp}_{33})\frac{d}{dr}-(\frac{\alpha^2_m}{r^2_k(n)}e^{kp}_{15}+\beta^2_n e^{kp}_{24})\}\Phi^k_r$$
$$+\{-\frac{\alpha_m}{r_k(n)}(e^{kp}_{31}+e^{kp}_{15})\frac{d}{dr}+\frac{\alpha_m}{r^2_k(n)}e^{kp}_{15}\}\Phi^k_\theta \quad (26)$$
$$+\{-\beta_n(e^{kp}_{32}+e^{kp}_{24})\frac{d}{dr}-\frac{\beta_n}{r_k(n)}e^{kp}_{32}\}\Phi^k_z$$
$$+\{-e^{kp}_{33}\frac{d^2}{dr^2}-\frac{e^{kp}_{33}}{r_k(n)}\frac{d}{dr}+(\frac{\alpha^2_m}{r^2_k(n)}e^{kp}_{11}+\beta^2_n e^{kp}_{22})\}\psi^{kp}=0$$

The general solution of Equations 23 through 26 is found by assuming that;

$$\begin{Bmatrix}\Phi_r\\ \Phi_\theta\\ \Phi_z\\ \psi^p\end{Bmatrix}_{k,n}=\begin{Bmatrix}A_{rmn}\\ B_{\theta mn}.A_{rmn}\\ B_{zmn}.A_{rmn}\\ B^p_{smn}.A_{rmn}\end{Bmatrix}_{k,n}.\exp(X_{mn}.r) \quad (27)$$

where A_{rmn}, $B_{\theta mn}$, B_{zmn}, B^p_{smn} and X_{mn} are constant coefficients for n^{th} sublayer of k^{th} lamina.

The above solution is valid for $r_k(n)-\frac{h_k(n)}{2}\le r\le r_k(n)+\frac{h_k(n)}{2}$ where $r_k(n)$ is the mean radius of n^{th} sub-layer of k^{th} lamina. Substituting 27 into Equations 23 through 26 and solving for X_{mn}'s will yield a polynomial of order six for nonpiezoelectric regions (sublayers) and of order eight for piezoelectric regions (sublayers). Upon determining X_{mn}'s, the constants $B_{\theta mn}$'s, B_{zmn}'s, and B^p_{smn}'s will be found by solving the linear algebraic equations obtained by substituting X_{mn}'s into Equations 24 through 26. The unknowns A_{rmn}'s will then be determined by imposing the necessary continuity conditions between each two adjacent sublayers. That is;

$$\begin{aligned}
(\Phi_r)_{k,n}\Big|_{r=r_k(n)+\frac{h_k(n)}{2}} &= (\Phi_r)_{k,n+1}\Big|_{r=r_k(n+1)-\frac{h_k(n+1)}{2}}\\
(\Phi_\theta)_{k,n}\Big|_{r=r_k(n)+\frac{h_k(n)}{2}} &= (\Phi_\theta)_{k,n+1}\Big|_{r=r_k(n+1)-\frac{h_k(n+1)}{2}}\\
(\Phi_z)_{k,n}\Big|_{r=r_k(n)+\frac{h_k(n)}{2}} &= (\Phi_z)_{k,n+1}\Big|_{r=r_k(n+1)-\frac{h_k(n+1)}{2}}\\
(\sigma_r)_{k,n}\Big|_{r=r_k(n)+\frac{h_k(n)}{2}} &= (\sigma_r)_{k,n+1}\Big|_{r=r_k(n+1)-\frac{h_k(n+1)}{2}} \quad (28)\\
(\tau_{rz})_{k,n}\Big|_{r=r_k(n)+\frac{h_k(n)}{2}} &= (\tau_{rz})_{k,n+1}\Big|_{r=r_k(n+1)-\frac{h_k(n+1)}{2}}\\
(\tau_{r\theta})_{k,n}\Big|_{r=r_k(n)+\frac{h_k(n)}{2}} &= (\tau_{r\theta})_{k,n+1}\Big|_{r=r_k(n+1)-\frac{h_k(n+1)}{2}}
\end{aligned}$$

where $h_k(n)$ is the thickness of n^{th} sublayer of k^{th} lamina. In addition, for piezoelectric regions (sublayers) there are two additional necessary continuity conditions as follows;

$$\begin{aligned}
(\psi)^p_{k,n}\Big|_{r=r_k(n)+\frac{h_k(n)}{2}} &= (\psi)^p_{k,n+1}\Big|_{r=r_k(n+1)-\frac{h_k(n+1)}{2}} \quad (29)\\
(D_r)^p_{k,n}\Big|_{r=r_k(n)+\frac{h_k(n)}{2}} &= (D_r)^p_{k,n+1}\Big|_{r=r_k(n+1)-\frac{h_k(n+1)}{2}}
\end{aligned}$$

4. NUMERICAL RESULTS AND DISCUSSIONS

The material properties of the piezoelectric layer considered here are those for a piezoelectric ceramic-PZT [7]:

Elastic constants;

$$[C]=\begin{bmatrix} 11.3 & & & & & \\ 7.43 & 13.9 & & & \text{sym.} & \\ 7.43 & 7.78 & 13.9 & & & \\ 0 & 0 & 0 & 2.6 & & \\ 0 & 0 & 0 & 0 & 2.56 & \\ 0 & 0 & 0 & 0 & 0 & 2.56 \end{bmatrix} \times 10^{10}\ \text{Pa} \quad (30a)$$

Piezoelectric constants;

$$[e]=\begin{bmatrix} 15.1 & 0 & 0 \\ -5.2 & 0 & 0 \\ -5.2 & 0 & 0 \\ 0 & 0 & 0 \\ 0 & 0 & 12.7 \\ 0 & 12.7 & 0 \end{bmatrix} \text{c.m}^{-2} \quad (30b)$$

Dielectric constants;

$$[\in]=\begin{bmatrix} 5.62 & 0 & 0 \\ 0 & 6.46 & 0 \\ 0 & 0 & 6.46 \end{bmatrix} \times 10^{-9}\ \text{F.m}^{-1} \quad (30c)$$

The material properties of the graphite-epoxy layer are [7];

$$\begin{aligned} &E_z = 76.8\times10^9\ \text{Pa} \quad , \quad E_r = E_\theta = 5.5\times10^9\ \text{Pa} \\ &G_{zr} = G_{z\theta} = 2.07\times10^9\ \text{Pa}, \quad G_{\theta r} = 1.4\times10^9\ \text{Pa} \\ &\nu_{zr} = \nu_{z\theta} = 0.34 \quad , \quad \nu_{\theta r} = 0.37 \end{aligned} \quad (31)$$

Two cases are considered in this study with a three-layered [P/90°/0°] panel, one with $\theta_0 = 45°$ and the other one with $\theta_0 = 22.5°$. In each case both the sensorial and actuating state responses due to outer pressure have been studied for the aforementioned laminates with the following geometric dimensions;

$$S \equiv \frac{R_0}{H} = 52 \quad , \quad \frac{L}{R_0} = 1 \quad (32)$$

where R_0 denotes the mean radius of the cylindrical panel, H is the panel thickness, and L is the panel length in z-direction (see Figure 1).

In Fourier's series, a few terms can give satisfactory results for the case studied (i.e., S = 52, $L/R_0 = 1$). Therefore 20 terms have been used throughout the analysis in each direction. In all cases, each lamina is divided into 5 sublayers, so the radial location $15\times\frac{(R-R_{in})}{H}$ will be shown in the figures with the numbers 0 to 15 for [P/90°/0°] laminates. When $\theta_0 = 45°$, the laminate will be referred to as the 45° - panel whereas when θ_0 is 22.5° it is said that the laminate is a 22.5° - panel.

Figure 3 shows the sensorial voltage distribution (voltage distribution when the piezoelectric layer is served as a sensor) across the thickness of the 45° - panel at θ = 22.5°. Similar

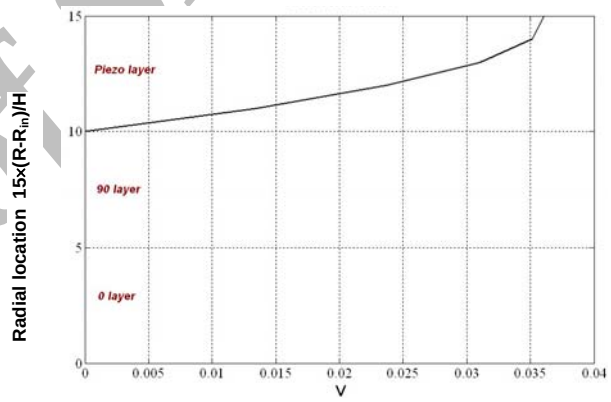

Figure 3. Through the thickness sensorial voltage distribution at the middle (i.e., at θ = 22.5°) of 45° - panel subjected to outer pressure.

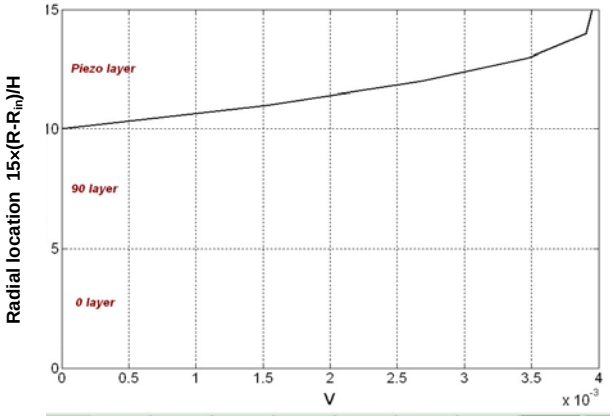

Figure 4. sensorial voltage distribution at the middle (i.e., at θ = 11.25°) of 22.5° - panel subjected to outer pressure.

results are presented for the 22.5° - panel in Figure 4. These figures illustrate the effect of θ_0 on the laminate sensitivity (maximum voltage measured on the piezoelectric layer when the structure is subjected to outer pressure). It can be seen that the 45° - panel is about 9 times more sensitive than the 22.5° - panel.

Figure 5 illustrates the voltage distribution across the thickness of the 45° - panel in which the piezoelectric layer is being used as an actuator. A Similar graph for the 22.5° - panel is presented in Figure 6. It is seen that in low actuating voltages the distribution becomes more nonlinear. Generally, it can be seen that if the panel angle θ_0 is increased and/or the actuating voltage is decreased the voltage variation across the thickness will be more nonlinear. So the linear assumption for voltage distribution should be considered with much more caution in high sensitive structures under low actuating voltages.

Figures 7 and 8 demonstrate the through-thickness distribution of radial stress σ_r for 45° - and 22.5° - panels in sensorial state. It is seen that the response of the 45° - panel to the outer pressure is about 5 times greater than that of the 22.5° - panel.

In Figures 9 and 10 the through-thickness

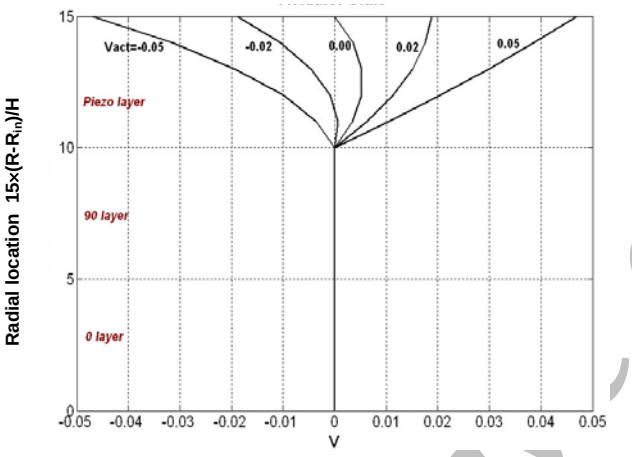

Figure 5. Actuator voltage distribution at the middle (i.e., at θ = 22.5°) of 45° - panel subjected to outer pressure.

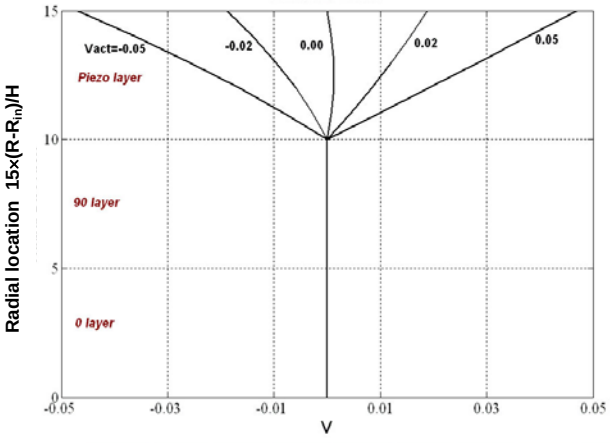

Figure 6. Actuator Voltage Distribution at the Middle (i.e., at θ = 11.25°) of 22.5° - Panel Subjected to Outer Pressure.

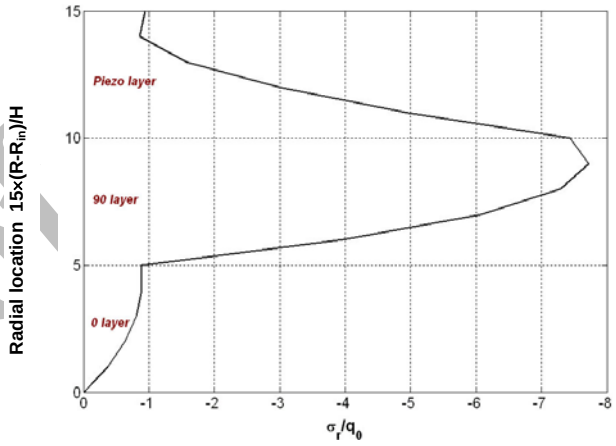

Figure 7. Through-thickness distribution of radial stress at the middle point (i.e., at θ = 22.5°) of 45° - Panel subjected to outer pressure.

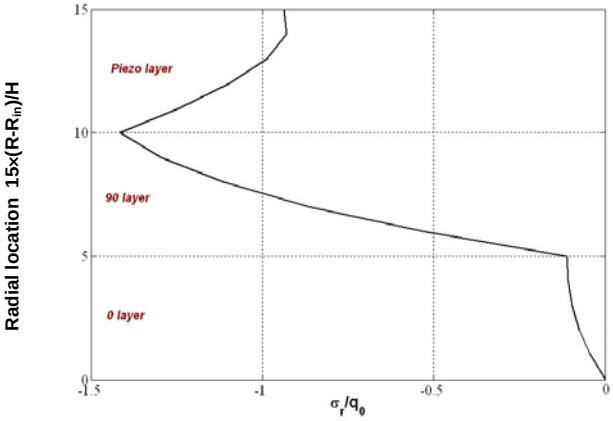

Figure 8. Through-thickness distribution of radial stress at the middle point (i.e., at θ = 11.25°) of 22.5° - panel subjected to outer pressure.

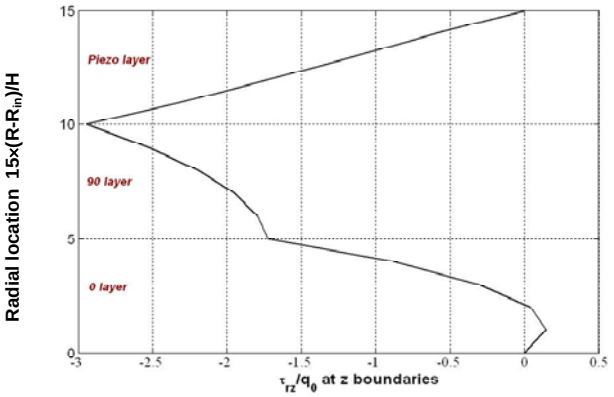

Figure 9. Through-thickness distribution of τ_{rz} at the longitudinal boundaries (with $\theta = 22.5°$) of 45° - panel subjected to outer pressure.

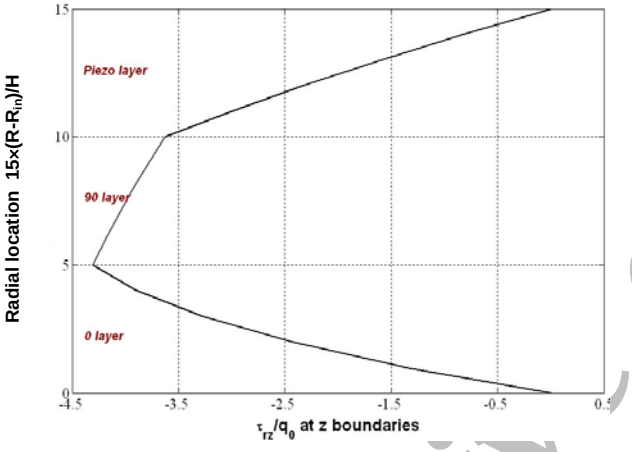

Figure 10. Through-thickness distribution of τ_{rz} at the longitudinal boundaries (with $\theta = 11.25°$) of 22.5° - panel subjected to outer pressure.

distributions of interlaminar shear stress τ_{rz} at the longitudinal boundaries (i.e., at z = 0 and z = $\frac{L}{R_0}$) are presented for 45°- and 22.5°-panels in sensorial state. Similar plots for $\tau_{r\theta}$ at the angular boundaries (i.e., at $\theta = 0$ and $\theta = \theta_0$) are shown in Figures 11 and 12. These figures clearly indicate that $\tau_{r\theta}$ in a sensorial state will be very large if the panel angle θ_0 is increased. This variation in stress levels directly affects the sensitivity of the structure as mentioned earlier.

Variations of radial stresses σ_r at the middle point of the panel in different actuating voltages are presented in Figures 13 and 14 for the 45° - and

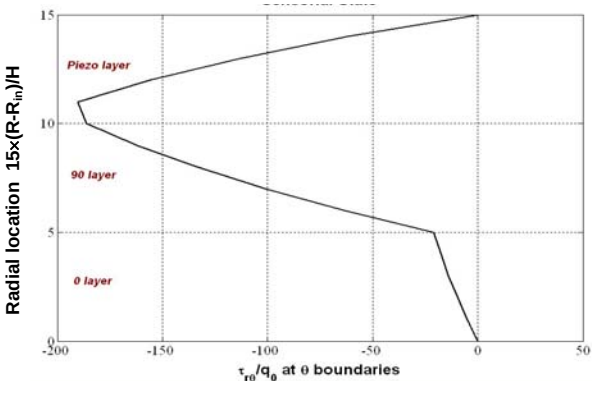

Figure 11. Through-thickness distribution of $\tau_{r\theta}$ at the angular boundaries (with z = L/2) of 45° - panel subjected to outer pressure.

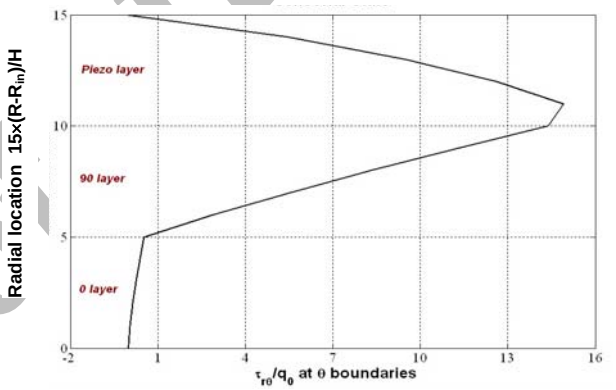

Figure 12. Through-thickness distribution of $\tau_{r\theta}$ at the angular boundaries (with z = L/2) of 22.5° - panel subjected to outer pressure.

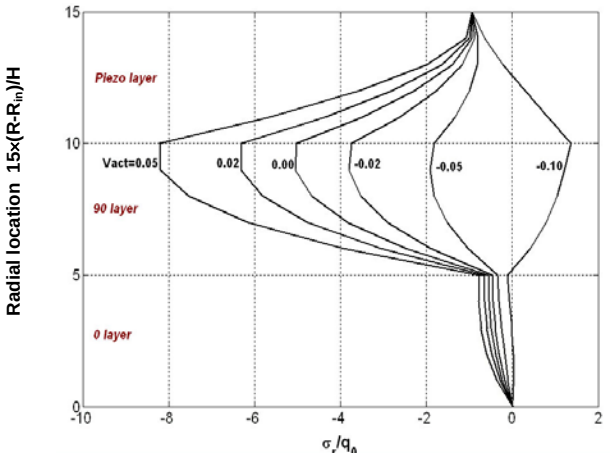

Figure 13. Variation of radial stress through the thickness at the middle point (i.e., at $\theta = 22.5°$) of 45° - panel subjected to outer pressure.

22.5°-panels, respectively. These figures demonstrate the great influence of the actuating lamina in controlling the radial stress through the thickness of the laminate. By comparing Figures 13 and 14 in the state of "0.00 V" actuating voltage with Figures 7 and 8 - in sensorial state - it can be seen that there are some differences between the maximum stresses and their distributions. These differences may be attributed to the differences between the characteristic behaviour of the piezoelectric layer in sensorial and actuating states.

Figures 15 and 16 show the variations of τ_{rz} at the longitudinal boundaries of 45° - and 22.5° - panels, respectively, in different actuating voltages. Those of $\tau_{r\theta}$ at the angular edges are presented in

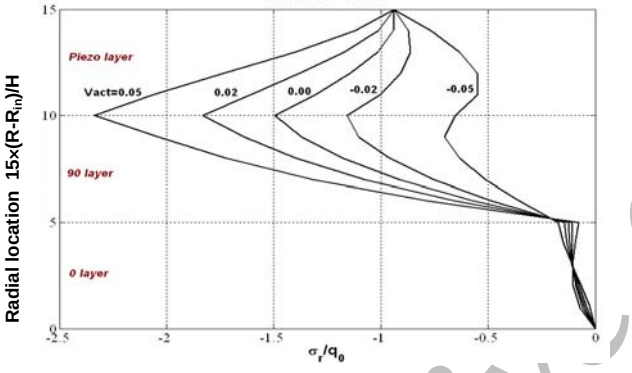

Figure 14. Variation of radial stress through-thickness at the middle point (i.e., at θ = 11.25°) of 22.5° - panel subjected to outer pressure.

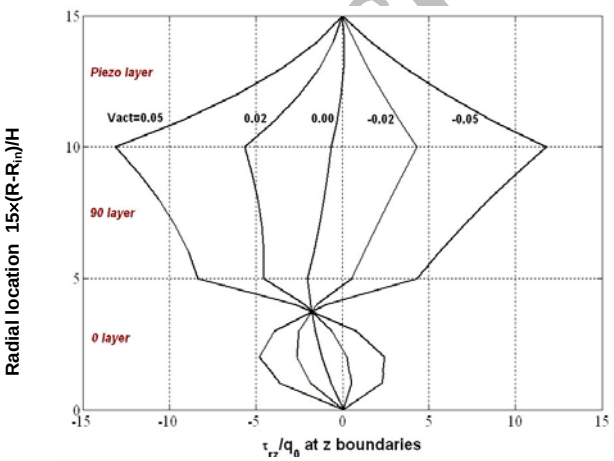

Figure 15. Variation of τ_{rz} through-thickness at the longitudinal boundaries (with z = L/2) of 45° - panel subjected to outer pressure.

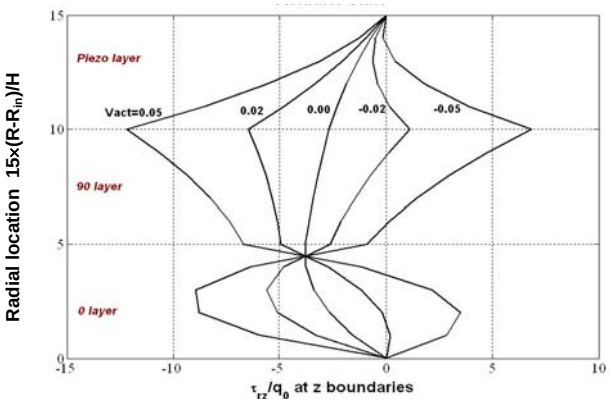

Figure 16. Variation of τ_{rz} through-thickness at the longitudinal boundaries (with z = L/2) of 22.5° - panel subjected to outer pressure.

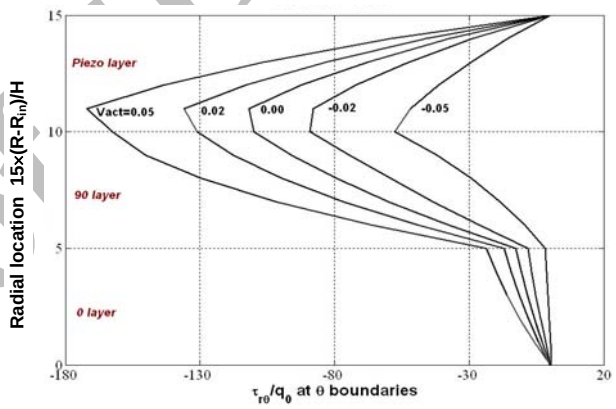

Figure 17. Variation of $\tau_{r\theta}$ through-thickness at the longitudinal boundaries (with z = L/2) of 45° - panel subjected to outer pressure.

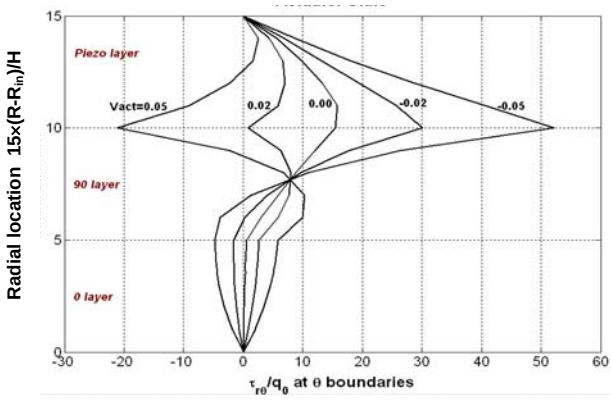

Figure 18. Variation of $\tau_{r\theta}$ through-thickness at the longitudinal boundaries (with z = L/2) of 22.5° - panel subjected to outer pressure.

Figures 17 and 18. Since the 45° - panel is much more sensitive than the 22.5° - panel, the actuating voltage will be more effective in controlling these stresses in the 45° - panel.

Finally, the through-thickness distributions of hoop stress σ_θ in different actuating voltages are presented in Figures 19 and 20. It can be seen that this stress is extremely affected by varying actuating voltages. By comparing these figures with Figures 13 through 18, it can be observed that by controlling any one of the stress components, one would be giving up the controlling of the remaining ones.

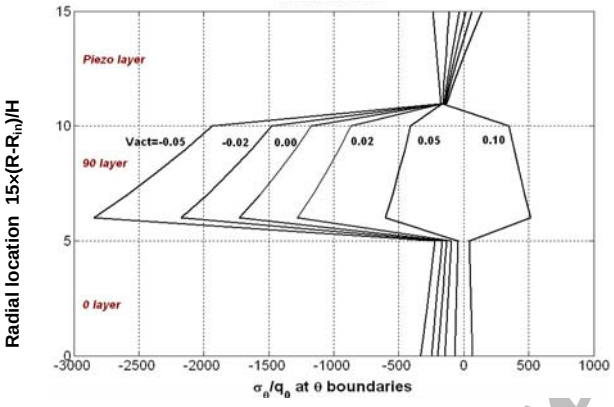

Figure 19. Through-thickness distribution of hoop stress at θ = 22.5° in different actuating voltages in the 45° - panel subjected to outer pressure.

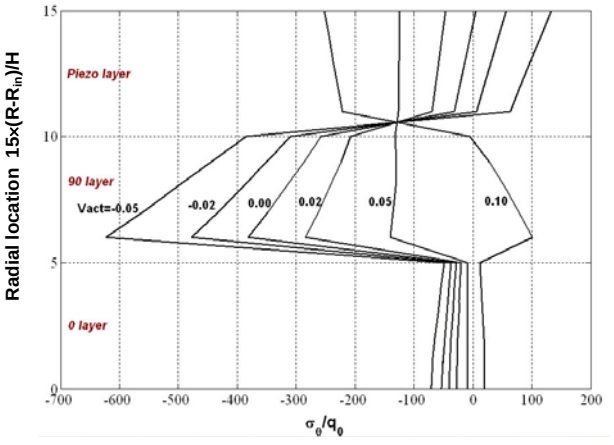

Figure 20. Through-thickness distribution of hoop stress at θ = 11.25° in different actuating voltages in the 22.5° - panel subjected to outer pressure.

5. CONCLUSIONS

A simple method for three-dimensional analysis of finite cross-ply laminated cylindrical panels with piezoelectric layers under uniform outer pressure loading and electrical excitation is presented. The panels are simply supported at four edges. The present work may provide an enhanced insight into the mechanical and electrical responses of such structures. The results are obtained for both direct and inverse piezoelectric effects. Numerical results are presented for three-layered finite circular cylindrical panels made of one piezoelectric layer and two orthotropic layers.

It is observed that the maximum radial stress may not occur in the outer or inner surfaces of the shell which, on the other hand, can be controlled by imposing different actuating voltages on the piezoelectric layers. Also, the amount of discontinuity of the in-plane stress σ_θ between the layers within a laminate can be controlled by changing the applied electric voltage appropriately. Another important result is that the linear assumption for voltage distribution in actuating states are acceptable only in thin piezoelectric layers -and high actuating voltages. If the layer is thick or the actuating voltage is high, the voltage distribution out through the thickness will be more nonlinear.

Also in cylindrical panels the sensitivity of the structures and consequently the actuating power of the structure depend directly and greatly on the panel angle θ_0 in both sensorial and actuating states. It is seen that as θ_0 increases, the panel is more sensitive and, consequently, behaves more effectively in an actuating state.

6. REFERENCES

1. Tauchert, T. R., "Plane Piezothermoelastic Response of a Hybrid Laminate-A Benchmark Problem", ***Composite Structures***, Vol. 39, (1997), 329-336.
2. Ding, H. J. and Chen, W. Q., "Three Dimensional Problems of Piezoelasticity", New York, Nova Science Publishers, (2001).

3. Chen, S., Soh, A. K., Long, Y. Q. and Yao, Z. H., A., "New 4-Node Quadrilateral FE Model with Variable Electrical Degree of Freedom for the Analysis of Piezoelectric Laminated Composite Plates", ***Composite Structures***, Vol. 58, (2002), 583-599.
4. Altay, G. A., and Dokmeci, M. C., "Some Comments on the Higher Order Theories of Piezoelectric, Piezothermoelastic and Thermopiezoelectric Rods and Shells", ***Int. J. Solids Struct.***, Vol. 40, (2003), 4699-4706.
5. Mannini, A. and Gaudenzi, P., "Multi-Layer Higher-Order Finite Elements for the Analysis of Free-Edge Stresses in Piezoelectric Actuated Laminates", ***Composite Structures***, Vol. 61, (2003), 271-278.
6. Mitchell, J. A. and Reddy, A., "Study of Embedded Piezoelectric Layers in Composite Cylinders", ***J. Appl. Mech.***, Vol. 62, (1995), 166-173.
7. Chen, C. Q. and Shen, Y. P., "Piezothermoelasticity Analysis for a Circular Cylindrical Shell under the State of Axisymmetric Deformation", ***Int. J. Eng. Sci.***, Vol. 34, No. 14, (1996), 1585-1600.
8. Chen, C. Q., Shen, Y. P., Liang, X., "Three-Dimensional Analysis of Piezoelectric Circular Cylindrical Shell of Finite Length", ***Acta Mech.***, Vol. 134, (1999), 235-249.
9. Chen, C. Q., Shen, Y. P., Wang, X. M., "Exact Solution of Orthotropic Cylindrical Shell with Piezoelectric Layers Under Cylindrical Bending", ***Int. J. Solid Structures***, Vol. 33, (1996), 4481-4494.
10. Wu, X. H., Chen, C. Q., Shen, Y. P., and Tian, X. G., A Higher-Order Theory for Functionally Graded Piezoelectric Shells, ***Int. J. Solids Struct.***, Vol.39, No.20, (2002), 5325-5344.
11. Wang, X. and Zhong, Z., "A Finitely Long Circular Cylindrical Shell of Piezoelectric/Piezomagnetic Composite under Pressuring and Temperature Change", ***Int. J Eng. Sci***., Vol. 41, (2003), 2429-2445.
12. Kapuria, S., Dumir, P. C. and Sengupta, S., "Exact Piezothermoelastic Axisymmetric Solution of a Finite Transversely Isotropic Cylindrical Shell", ***Computers and Structures***, Vol. 61, No. 6, (January 1996), 1085-1099.
13. Ossadzow, C. and Touratier, M., "A Multilayered Piezoelectric Shell Theory", ***Composites Science and Technology***, (2004), [in press].
14. Wu, X. H., Shen, Y. P. and Chen, C., "An Exact Solution for Functionally Graded Piezothermoelastic Cylindrical Shell as Sensors or Actuators", ***Materials Letters***, Vol. 57, (2003), 3532-3542.
15. Ma, L. F., Chen, Y. H. and Zhang, S. Y., "On the Explicit Formulations of Circular Tube, Bar and Shell of Cylindrically Piezoelectric Material Under Pressuring Load", ***Int. J. of Eng. Sci.***, Vol. 39, (2001), 369-385.
16. Ashida, F., "Reduction of Applied Electric Potential Controlling Thermoelastic Displacement in a Piezoelectric Actuator", ***Arch. Appl. Mech.***, Vol. 69, (1999), 443-454.
17. Kapuria, S., Sengupta, S. and Dumir, P. C., "Three-Dimensional Piezothermoelastic Solution for Shape Control of Cylindrical Panel", ***J. Thermal Stresses***, Vol. 20, (1997), 67-85.
18. Ashida, F. and Tauchert, T. R., "Control of Transient Thermoelastic Displacement in a Composite Disk", ***J. Thermal Stresses***, Vol. 25, (2002), 99-121.
19. Ootao, Y. and Tanigawa, Y., "Control of Transient Thermoelastic Displacement of an Angle-Ply Laminated Cylindrical Panel Bonded to a Piezoelectric Layer", ***Appl. Math. and Computations***, Vol. 148, (2004), 263-286.
20. Tzou, H. S., "Piezoelectric Shells: Distributed Sensing and Control of Continua", Kluwer Acad. Pub., Boston/Dordrecht, (1993).
21. Tiersten, H. F., "Linear Piezoelectric Plate Vibrations", Plenum Press, New York, (1969).
22. Rogacheva, N. N., "The Theory of Piezoelectric Shells and Plates", CRC Press, (1994).
23. Xu, K. and Noor A. K., "Three-Dimensional Analytical Solutions for Coupled Thermoelectroelastic Response of Multilayered Cylindrical Shells", ***AIAA J.***, Vol. 34, No. 4, (1996), 802-812.
24. Reddy, J. N., "On Laminated Composite Plates with Integrated Sensors and Actuators", ***Engineering Structures***, Vol. 21, (1999), 568-593.
25. Tauchert, T. R., Ashida, F., Noda, N., Adali, S. and Verijenko, V., "Developments in Thermopiezoelasticity with Relevance to Smart Composite Structures", ***Composite Structures***, Vol. 48, (2000), 31-38.
26. Giacovazzo, C., Monaco, H. L., Artioli, G., Viterbo, D. and Ferraris, G., "Fundamentals of Crystallography", Oxford Science Pub., (1992).
27. Nye, N. Y., "Physical Properties of Crystals", Oxford University Press, (1972).
28. Cady, W. G., "Piezoelectricity", Dover Pub., New York, (1964).
29. Ikeda, T., "Fundamentals of Piezoelectricity", Oxford University, (1990).
30. Herakovich, C. T., "Mechanics of Fibrous Composites", John Wiley and Sons, Inc., (1998).